

Published in final edited form as:

*Invest Ophthalmol Vis Sci.* 2007 June ; 48(6): 2685–2694.

## Age-Related Cataracts in $\alpha 3\text{Cx}46$ -Knockout Mice Are Dependent on a Calpain 3 Isoform

Yajun Tang<sup>1</sup>, Xiangyang Liu<sup>1,2</sup>, Rebecca K. Zoltoski<sup>2,3</sup>, Layne A. Novak<sup>4,5</sup>, R. Antonio Herrera<sup>1</sup>, Isabelle Richard<sup>6</sup>, Jer R. Kuszak<sup>4,5</sup>, and Nalin M. Kumar<sup>1</sup>

<sup>1</sup>Department of Ophthalmology and Visual Sciences, University of Illinois at Chicago, Chicago, Illinois;

<sup>3</sup>Department of Biological Sciences, Illinois College of Optometry, Chicago, Illinois;

<sup>4</sup>Department of Ophthalmology, Rush University Medical Center, Chicago, Illinois;

<sup>5</sup>Department of Pathology, Rush University Medical Center, Chicago, Illinois;

<sup>6</sup>Généthon, Évry, France.

### Abstract

**Purpose**—Previous studies have demonstrated that in  $129\alpha 3\text{Cx}46^{-/-}$  mice, age-related nuclear cataract is formed. In the present study, a more in vivo-relevant model was generated to test the hypothesis that the calpain 3 gene is involved in age-related nuclear cataractogenesis in  $\alpha 3\text{Cx}46$  knockout mice.

**Methods**—To test the hypothesis that the calpain 3 gene is involved in age-related nuclear cataractogenesis in  $\alpha 3\text{Cx}46$  knockout mice,  $129\alpha 3\text{Cx}46^{-/-}$  and  $\text{CAPN}3^{-/-}$  mice were mated to generate homozygous double-knockout (dKO) mice. Lenses from the mice were examined by visual observation, laser scan analysis, and histologic and biochemical methods.

**Results**—In the absence of the  $\text{CAPN}3$  gene, the formation of a cataract was delayed, and its appearance was changed to a more diffuse, pulverulent type. Unlike in the  $129\alpha 3\text{Cx}46^{-/-}$  mouse, cleavage of  $\gamma$ -crystallin was not detected in the dKO mouse. In both  $129\alpha 3\text{Cx}46^{-/-}$  and dKO mice, total  $\text{Ca}^{2+}$  increased.

**Conclusions**—The present study shows for the first time that calpain 3 is necessary for the formation of age-dependent nuclear cataracts in  $\alpha 3\text{Cx}46^{-/-}$  mice. Evidence that the calpain 3 gene is directly involved in, or part of the pathway that leads to,  $\gamma$ -crystallin cleavage is presented. These results are consistent with the hypothesis that the loss of  $\alpha 3\text{Cx}46$  leads to increased levels of  $\text{Ca}^{2+}$  ions, and this increase activates the  $\text{CAPN}3$  isoform, Lp82/85, which results in the formation of a nuclear cataract.

Gap junctions consist of two hexameric structures of connexin (Cx) molecules called connexons, which are located in the plasma membranes of two neighboring cells. So far, more than 20 connexin genes have been identified in vertebrates.<sup>1,2</sup> Three connexin genes are expressed in the vertebrate lens:  $\alpha 1\text{Cx}43$  connexin in epithelial cells<sup>3</sup> and  $\alpha 3\text{Cx}46$  and  $\alpha 8\text{Cx}50$  connexin in fiber cells.<sup>4,5</sup>

Corresponding author: Nalin M. Kumar, Department of Ophthalmology and Visual Sciences, University of Illinois at Chicago, 1855 West Taylor Street, Chicago, IL 60612; nalin@uic.edu.

<sup>2</sup>Contributed equally to the work and therefore should be considered equivalent authors.

Disclosure: **Y. Tang**, None; **X. Liu**, None; **R.K. Zoltoski**, None; **L.A. Novak**, None; **R.A. Herrera**, None; **I. Richard**, None; **J.R. Kuszak**, None; **N.M. Kumar**, None

Previous studies have demonstrated that, in a  $129\alpha3Cx46$  KO mouse, an age-related nuclear cataract is formed that resembles cataracts in humans.<sup>6-8</sup> In both the mouse model and humans, increased levels of calcium ions (human cortical cataracts) and  $\gamma$ -crystallin cleavage (senile cataracts in humans) have been observed.<sup>8-11</sup> The protease responsible for cleavage of  $\gamma$ -crystallin is not known, but a lens-specific isoform of calpain3 (CAPN3) has been implicated in the mouse model.<sup>8</sup> Furthermore, mutations in the  $\alpha3Cx46$  gene have been linked to congenital cataract in humans.<sup>12,13</sup>

Calpains are a group of calcium-activated cysteine proteases. Unregulated  $Ca^{2+}$ -mediated proteolysis of essential lens proteins by calpains may be a major contributor to some forms of cataract in both animals and humans, and drugs that inhibit calpains may be useful for prevention of cataracts.<sup>14</sup> In human cortical cataracts, total lens  $Ca^{2+}$  increases by an average of 20-fold to give millimolar levels of the ion, far in excess of those necessary to overactivate calpains.<sup>15</sup>

There are at least four calpains in the lens: calpain 1 ( $\mu$ -calpain), calpain 2 (m-calpain), calpain 10, and Lp82/85.<sup>14</sup> Lp82 and Lp85 are lens-specific splice variants of calpain 3 (CAPN3).<sup>16</sup> Lp82 is the dominant form of calpain in the young mouse lens<sup>17</sup> and is localized to both nuclear and cortical regions of the lens from the newborn mice.<sup>18</sup> It has been demonstrated in  $\alpha3Cx46^{-/-}$  mouse lenses that the  $Ca^{2+}$  level is increased, resulting in activation of Lp82 that ultimately leads to  $\gamma$ -crystallin proteolysis.<sup>8,9</sup> Lp82-mediated cataractogenesis in rodent lenses has also been reported on calcium ionophore A23187 or selenite injections.<sup>19,20</sup> CAPN3<sup>-/-</sup> mice show a mild progressive muscular dystrophy that affects a specific group of muscles.<sup>21</sup> It has been reported that these CAPN3-knockout mice develop a lens normally, and no cataracts are visible.<sup>18</sup>

Because age-related cataracts are the leading cause of blindness worldwide, therapeutic, nonsurgical strategies would have a profound impact on the quality of life. A better understanding of the mechanism by which cataracts are formed would make this goal more readily achievable.

The objective of this study was to determine the role of protease calpain 3 and  $\gamma$ -crystallin degradation in cataract formation in the  $\alpha3Cx46^{-/-}$  mice. We generated a  $\alpha3Cx46$ /CAPN3 double-knockout (dKO) mouse to investigate the effects of both  $\alpha3Cx46$  and calpain 3 genes on lens function.

## Materials and Methods

### Generation of $129\alpha3Cx46$ and CAPN3 Homozygous dKO Mice

The mice used in this study have been described elsewhere.<sup>6,21</sup>  $129Sv\alpha3Cx46^{-/-6}$  and  $129SvCAPN3^{-/-21}$  mice were mated to generate heterozygotes. The heterozygotes were then backcrossed, and the genotypes were analyzed by PCR until homozygous dKO mice were obtained.

All animal experiments were performed according to the ARVO Statement for the Use of Animals in Ophthalmic and Vision Research, as well as the guidelines established by the Animal Care Committee of the University of Illinois at Chicago.

### Genotyping of Mice

To genotype the mice, we used three primers for PCR to determine the presence of wild-type (WT) or  $\alpha3Cx46$  disrupted alleles, as previously described.<sup>6</sup> The predicted PCR product sizes are 405 bp for the  $\alpha3Cx46$ WT gene and 500 bp for the  $\alpha3Cx46$ -KO gene.

Two pairs of primers were used for PCR, to determine the presence of WT or CAPN3 disrupted alleles, as described elsewhere.<sup>21</sup> The predicted PCR product sizes are 350 bp for CAPN3 WT alleles and 650 bp for the CAPN3 gene disrupted alleles.

### Optical Quality Analysis

Mice (7 to 8 weeks old) were group housed, with free access to standard laboratory chow and water in a normal 12-hour light–dark schedule. Mice were wild-type ( $n = 8$ ),  $\alpha 3\text{Cx}46^{-/-}$  ( $n = 4$ ), CAPN3<sup>-/-</sup> ( $n = 8$ ), or CAPN3 and  $\alpha 3$  dKO ( $n = 8$ ).

Immediately after death induced with an overdose of euthanizing solution (Euthasol; Butler Co., Alsip, IL), the eyes were enucleated, and the lenses were removed into culture medium (M199; Invitrogen-Gibco, Grand Island, NY). The lenses were each suspended by the equatorial rim on a beveled washer in a specially designed two-chambered glass and silicon rubber cell. Both surfaces of the lens were bathed in a culture medium (25 mL) consisting of M199 with Earle's salts and 8% fetal bovine serum.

Average back vertex distance (BVD) and variability in BVD were quantified on the right eye lens from each animal by an in vitro assay system (Scantox; Harvard Apparatus Inc., Hollister, MA), performed as described.<sup>22-24</sup> The system consists of a collimated laser source that projects a 0.5-mm-wide laser beam onto a mirror mounted on a carriage assembly at 45°. The mirror reflects the laser beam directly up through the lens. The mirror carriage is controlled by a position motor connected to a drive screw that permits a series of parallel laser beams to be passed in defined steps across the lens. A digital camera captures the actual position and slope of the laser beam transmitted at each step. Eight laser beams were passed at equal increments, defined by dividing the equatorial diameter of the lens by the number of steps. In addition, the lens was rotated in 30° increments until the entire lens was scanned. This methodology enables the curvature of the lens to be accounted for by the multiple laser passes at known longitudinal and latitudinal positions. On completion of all steps, the captured data were used to calculate the average BVD, as well as the variability of the BVD.

BVD is defined as measurements of the laser beam from the rear surface of the lens to the focal point. Repeated measurements of BVD indicate instrument reproducibility within 0.32% of BVD. Changes in this distance with beam position are predominantly the result of longitudinal spherical aberration. Variability in BVD, defined as the average standard error of the mean of the BVD of all laser scans, in each lens is an indication of the fine-focusing capabilities. This parameter is affected by naturally occurring or pathologically induced irregularities in the lens fibers.

Statistical analysis to determine whether significant differences were present between the BVD and variability in BVD were performed by Mann-Whitney *t*-test for independent samples. A difference reaching at least  $P \leq 0.05$  was considered significant.

### Histologic Analysis

Lenses from mice were dissected and examined by stereo microscope (Carl Zeiss Meditec, Thornwood, NY), as described.<sup>25</sup> Mouse lenses (between 7.5 and 8 weeks old) from WT,  $\alpha 3\text{Cx}46^{-/-}$ , CAPN3<sup>-/-</sup>, and  $\alpha 3\text{Cx}46/\text{CAPN3}$  dKO mice were fixed in 2.5% glutaraldehyde in 0.07 M sodium cacodylate buffer (pH 7.2) at room temperature for 18 to 24 hours. After overnight washing in 0.2 sodium cacodylate buffer, the lenses were postfixed in 1% aqueous osmium tetroxide at 4°C overnight, then washed in cacodylate buffer and dehydrated through a graded ethanol series to propylene oxide. Lenses were infiltrated and embedded flat in epoxy resin. One-micrometer-thick sections were cut along the optic axis with a glass knife. Sections were mounted on glass slides and stained with a dilute mixture of methylene blue and azure

II. Light micrographs were taken on a photographic microscope (Vanox AHBS3; Olympus America, Inc., Melville, NY) equipped with a 35-mm camera.

### Lens Homogenization and Western Blot Analysis

Lenses were dissected from both eyes of WT,  $\alpha3Cx46^{-/-}$ ,  $CAPN3^{-/-}$ ,  $\alpha3Cx46^{-/-}$   $CAPN3^{+/-}$  heterozygote, and  $\alpha3Cx46/CAPN3$  dKO mice using a posterior approach. Wet weights were determined. Lenses were homogenized in 200  $\mu$ L of PBS, and protein concentration was measured in a bicinchoninic acid protein assay (BCA, Protein Assay Kit; Pierce, Rockford, IL). Between 5 and 200  $\mu$ g of total protein were analyzed on either 15% or 10% to 20% gradient Tris-glycine SDS-polyacrylamide gels (Invitrogen, Carlsbad, CA). Western blot analysis was performed as previously described,<sup>26</sup> using anti- $\gamma$ ,  $\alpha A$ , or  $\alpha B$ -crystallin, primary antibodies,<sup>27</sup> a kind gift from Usha Andley (Washington University, St. Louis, MO). The  $\beta$ -crystallin antibody was obtained commercially (QED Bioscience Inc., San Diego, CA). The bound antibodies were detected by chemiluminescence (Supersignal West Pico; Pierce), using a goat anti-rabbit or goat anti-mouse horseradish peroxidase secondary antibody (Bio-Rad Laboratory, Hercules, CA).

### Measurement of Ion Concentrations

Ion concentrations were measured as previously described.<sup>8</sup> Briefly, lenses from WT,  $\alpha3Cx46^{-/-}$ ,  $CAPN3^{-/-}$ , or dKO mice were dissected and vacuum dried for 2 days. Pairs of dry lenses were weighed and solubilized in 100  $\mu$ L of 2% nitric acid for 12 hours at 37°C. Nanopure water was added to a final volume of 5 mL. The content of calcium, sodium, magnesium, and potassium was determined by emission spectrometry with a coupled plasma-optical emission spectrometer (ICP-OES) at the University of California at San Diego. All measurements were normalized to dry lens weight.

## Results

### Generation of a $\alpha3Cx46/CAPN3$ dKO Mouse

129Sv  $\alpha3Cx46^{-/-6}$  and  $CAPN3^{-/-21}$  mice were mated to generate  $\alpha3Cx46^{+/-}/CAPN3^{+/-}$  mice. The offspring were mated to generate homozygous dKO mice. PCR using genomic DNA isolated from the tails was used for genotyping the offspring. In the homozygous  $\alpha3Cx46^{-/-}/CAPN3^{-/-}$  mice, dKO, both  $\alpha3Cx46^{-/-}$  allele and  $CAPN3$ -disrupted allele were detected by PCR and WT  $\alpha3Cx46$  allele and WT  $CAPN3$  were absent (data not shown).

### Effect on Lens Weight and Water Content of the Absence of the $\alpha3Cx46$ or $CAPN3$ Gene

The wet and dry weight and water content of the lenses from WT,  $\alpha3Cx46^{-/-}$ ,  $CAPN3^{-/-}$ , and dKO mice from the age of 4 weeks to 24 weeks was measured (Fig. 1). No significant change in the lens wet weight was detected (Fig. 1A). Though the average lens dry weight from  $\alpha3Cx46^{-/-}$  was less than WT littermates after 6 months, this difference was within the SD (Fig. 1B). Thus, the growth of the lens is not affected by the lack of the  $\alpha3Cx46$  or  $CAPN3$  gene. Lens water content was estimated by the difference in wet and dry lens weight. Though there is a trend toward greater water content in  $\alpha3Cx46^{-/-}$  mice (Fig. 1C), differences were not significant.

### Cataract Formation in the Lenses of dKO Mice

$\alpha3Cx46^{-/-}$  mice develop nuclear cataracts that increase in size and intensity with increasing age. Using a dissection microscope, a nuclear cataract was visible beginning at 2 weeks of age consistent with previous observations.<sup>6,7,8</sup> This is in contrast to the lenses of the dKO mice, which do not have a visible cataract, from birth until at least 5 weeks of age (Fig. 2). In these dKO mice, a slight opacity can be observed at 5 weeks that remains relatively constant in size,

location, and intensity up to 7.5 weeks. At 8 weeks there is a dramatic increase in size of a diffuse, powdery nuclear opacity and this was fully developed by 11 weeks. Although the nuclear cataract observed in the dKO lenses was larger than that found in the  $\alpha 3\text{Cx}46^{-/-}$  lenses, it never extended to the outer cortex. The cataract pattern of the heterozygote  $\alpha 3\text{Cx}46^{-/-}/\text{CAPN}3^{+/-}$  mice was similar to  $\alpha 3\text{Cx}46^{-/-}$  mice (Fig. 2), suggesting that the delay of cataract formation requires both alleles of calpain 3 to be disrupted.

### Optical Quality of the dKO and CAPN3<sup>-/-</sup> Lens

A laser-based in vitro assay system (Scantox; Harvard Apparatus) was used to measure the average BVD. To obtain lenses large enough (>2 mm diameter) to permit multiple passes of the laser, 7- to 8-week lenses from WT,  $\alpha 3\text{Cx}46^{-/-}$ , CAPN3<sup>-/-</sup>, and dKO mice were used for these experiments.

Because of a central opacity, none of the lenses from the  $\alpha 3\text{Cx}46^{-/-}$  could be analyzed with the laser scanner. However, the lenses from wild-type, CAPN3<sup>-/-</sup> and dKO mice were relatively clear and were able to be scanned. A representative laser scan from each of the three groups is shown in Figure 3 and a summary is shown in Table 1. In the wild-type lenses, the lower BVD indicates that the laser beams came to a sharper focus than in either of the knockout groups. Moreover, a significant increase in the BVD and variability in BVD was observed in both the CAPN3<sup>-/-</sup> and dKO groups compared with wild-type. Thus, disruption of CAPN3 gene causes both changes in the longitudinal spherical aberration (as indicated by the larger BVD) as well as a loss of fine focusing power (as indicated by the greater BVD variability). However, the effect on the dKO lens longitudinal spherical aberration was smaller than observed in lenses from the CAPN3<sup>-/-</sup> mice (Table 1).

### Histologic Analysis of Lenses

Under a stereo dissection microscope, all the lenses had typical gross structure with normal anterior and posterior Y sutures. Light microscopy (LM) examination of thick sections obtained along the visual axis showed that the layering of nuclei in the differentiation zone of the anterior epithelium in the  $\alpha 3\text{Cx}46^{-/-}$ , CAPN3<sup>-/-</sup>, and dKO lenses was different from the wild-type lenses (Fig. 4).

The layering of the nuclei of the fiber cells in these knockout lenses past the equatorial region, indicates that the rotation and the elongation of the differentiating fiber cells may be delayed in the dKO and possibly further delayed in the  $\alpha 3\text{Cx}46$ -knockout mice. In addition, the differentiation process (degradation of organelles) may also be delayed. However, an alteration in the organization of the cells in the differentiation zone of the epithelium was more evident in the  $\alpha 3\text{Cx}46^{-/-}$  lenses. Although the epithelial cells appear to rotate and elongate normally to form the lens fiber this occurred past the equatorial region. This contrasts with the WT lenses where this process occurs at the equatorial region. This delayed entry into the differentiation process resulted in improperly elongating cells in the outer regions of the cortex. Although the cells eventually elongate, the cell shape appears to be abnormal.

In the CAPN3<sup>-/-</sup> lens, an alteration in the epithelium differentiation zone was also observed, but to a lesser extent, with the shape of the fiber being relatively normal in the fiber elongation areas of the lens outer cortex. Cells past this point of differentiation appear to be normal at the LM level. The differentiation zone of the dKO also showed this slight delay, but again the elongation in the outer cortex of the lens appeared normal.

### Lack of $\gamma$ -Crystallin Cleavage in the dKO Lens

It has been demonstrated that a 11 kDa  $\gamma$ -crystallin cleavage product was correlated with the formation of the nuclear cataract in  $\alpha 3\text{Cx}46^{-/-}$  mice.<sup>6,7</sup> In the present study, the processing

of the different crystallins was analyzed during the onset of cataract formation in dKO mice. In contrast to the 11-kDa  $\gamma$ -crystallin fragment observed in  $\alpha 3\text{Cx}46^{-/-}$  mice, cleavage products of  $\gamma$ -crystallin were not detected in WT,  $\text{CAPN}3^{-/-}$ , or dKO mice by Coomassie blue staining or by Western blot analysis (Fig. 5). Analysis of total lens homogenate using antibodies specific for  $\alpha$ A- or  $\beta$ -crystallin did not reveal significant differences between WT,  $\alpha 3\text{Cx}46^{-/-}$ ,  $\text{CAPN}3^{-/-}$ , and dKO mice (Fig. 5C). However, Western blot analysis for  $\alpha$ B crystallin, indicated that in addition to  $\gamma$ -crystallin cleavage, there was a cleavage of the  $\alpha$ B crystallin that was unique to the  $\alpha 3\text{Cx}46^{-/-}$  mice and was age dependent (Fig. 5C). The significance, if any, of the  $\alpha$ B crystallin cleavage is not known.

### Effect of Loss of $\alpha 3\text{Cx}46$ and $\text{CAPN}3$ Genes on Ca Ion Levels in the Lens

An increase in  $\text{Ca}^{2+}$  ion levels has been reported to occur between 1 and 4 weeks in the lenses of  $\alpha 3\text{Cx}46^{-/-}$  mice.<sup>8</sup> Because an optical irregularity can be observed beginning at 5 weeks in the dKO, alterations in calcium homeostasis in these mice was investigated. The  $\text{Ca}^{2+}$  ion levels were measured for the mice at several different ages (4, 5, 8, 11 and 16 weeks). Lenses from either  $\alpha 3\text{Cx}46^{-/-}$  and dKO mice exhibited a dramatic increase in the levels of  $\text{Ca}^{2+}$  (Fig. 6A) with no marked change in the levels of  $\text{Mg}^{2+}$  and  $\text{K}^{+}$  ions at the same ages (Figs. 6C, 6D). However, there was a significant increase in  $\text{Na}^{+}$  ions only in the lenses from dKO mice (Fig. 6B). Lenses from WT and  $\text{CAPN}3^{-/-}$  mice at identical ages had similar ion levels to each other, with the  $\text{Ca}^{2+}$  ion levels being significantly lower than found in the  $\alpha 3\text{Cx}46^{-/-}$  or dKO lenses.

### Discussion

In a previous study,<sup>8</sup> a lens calpain 3 isoform was implicated in the formation of a cataract in  $\alpha 3\text{Cx}46$  knockout mice. However, this study used an in vitro organ culture system as well as calpain inhibitors. In the present study, we have extended these observations using an in vivo model. In this model, a dKO in which both the  $\alpha 3\text{Cx}46$  and  $\text{CAPN}3$  genes were disrupted in mice was generated. Our data indicated that calpain 3 activity is required for the timing and formation of the nuclear cataract in the  $\alpha 3\text{Cx}46^{-/-}$  mouse that begins 2 weeks after birth. In contrast to  $\alpha 3\text{Cx}46^{-/-}$  mice, dKO mice did not have observable opacities until at least 5 weeks after birth. There was a dramatic increase in the extent of the cataract between 8 and 11 weeks in lenses from the dKO mice but the opacity remained diffuse and had a “powdery” appearance. This is probably because of the lack of  $\gamma$ -crystallin cleavage in the dKO mouse that is detected in the  $\alpha 3\text{Cx}46^{-/-}$  mouse. This suggests that the calpain 3 gene is directly involved in, or part of the pathway that leads to,  $\gamma$ -crystallin cleavage.

It was reported in a previous study that the severity of the nuclear cataract in  $\alpha 3\text{Cx}46^{-/-}$  lenses was dependent on the strain background and correlated to the amount of cleaved  $\gamma$ -crystallin.<sup>7</sup> In contrast to the 129 strain background, no significant  $\gamma$ -crystallin cleavage in  $\alpha 3\text{Cx}46^{-/-}$  lenses in the C57BL/6J strain background was detected.<sup>7</sup> An isoform of calpain 3, Lp82/85, was suggested to lead to  $\gamma$ -crystallin cleavage.<sup>8</sup> The calpain3 gene is identical in both 129 and C57BL/6J strains of mice.<sup>21</sup> The lack of  $\gamma$ -crystallin cleavage in  $\alpha 3\text{Cx}46^{-/-}$  lenses in a C57BL/6J strain background could be because of, first, the calcium concentration never reaching a sufficiently high levels to activate Lp82/85. To activate Lp82, calcium needs to reach a critical level ( $\sim 1 \mu\text{M}$ ).<sup>8,9</sup> Measurement of the intracellular calcium concentrations by injection of FURA2 into the fiber cells of the lenses indicates that in 129 wild-type lenses the calcium concentration varies from 700 nM in the center to 300 nM at the surface.<sup>9</sup> This contrasts with the 129  $\alpha 3\text{Cx}46^{-/-}$  lenses where calcium accumulates to  $\sim 2 \mu\text{M}$  in the central fibers which should be sufficient to activate Lp82.<sup>9</sup> Second were unknown modifier gene(s) present in C57BL/6J strain but not in the 129 strain that potentially inhibit the cleavage of  $\gamma$ -crystallin caused by a loss of the  $\alpha 3\text{Cx}46$  gene in lenses. Alternatively, unknown gene products in the 129 strain possibly activate protease(s), or modify its activity, and leading ultimately to

cleavage of  $\gamma$ -crystallin. A thorough genomic and proteomic study of the differences of the mRNA and proteins between these two genetic background strains may clarify the phenotypic differences between these two strains.

In the present study, Western blot analysis for  $\alpha$ B crystallin indicated that in addition to  $\gamma$ -crystallin cleavage, there were cleavage fragments of the  $\alpha$ B crystallin that were unique to the  $\alpha$ 3C $\times$ 46<sup>-/-</sup> mice and were age dependent. However, although  $\alpha$ B crystallin cleavage was detected in the lenses of dKO mice, the smallest cleaved form of the  $\alpha$ B crystallin was not detected (Fig. 5C). The function of  $\alpha$  crystallin as a chaperone protein that prevents denaturation and aggregation of crystallins in vitro<sup>28</sup> and in vivo<sup>29</sup> has been described. Degradation of the C terminus of  $\alpha$ B crystallin may reduce their chaperone function.<sup>30</sup> In rat lens, in vitro proteolysis of  $\alpha$ B crystallin by either m-calpain or Lp82 was observed.<sup>31</sup> Cleavage fragments of  $\alpha$ B crystallin have also been detected in human cataracts.<sup>32</sup> A previous study determined that the relative ratio between the smallest cleaved form of  $\alpha$ B crystallin to its intact form was greater in the 129 $\alpha$ 3C $\times$ 46<sup>-/-</sup> mice than in the C57BL/6J  $\alpha$ 3C $\times$ 46<sup>-/-</sup> mice, and also correlated with the degree of opacity in the mixed background (129 $\times$ C57BL/6J)  $\alpha$ 3C $\times$ 46<sup>-/-</sup> mouse lenses.<sup>7</sup> Thus, the lack of the smallest cleaved forms of  $\alpha$ B crystallin in dKO mice may also contribute to the delayed cataract formation and the decreased severity of the cataract in dKO mice that was observed in the present study.

Laser scan analysis of lenses of 7.5-week-old dKO mice indicated that there was loss of focusing power with spherical aberrations when compared to wild-type mice. Similar analysis of lenses of  $\alpha$ 3C $\times$ 46<sup>-/-</sup> mice was not possible because of a dense nuclear cataract. Histologic analysis suggested that there was an alteration in the differentiation program of the dKO mouse as indicated by the presence of nuclei past the equator, and this correlated with the observed optical changes. These optical and histologic changes are probably related to the loss of the calpain 3 gene, because they were also observed in the CAPN3<sup>-/-</sup> lenses. The elongation of the fibers appeared to be normal. However, the observed pattern of the nuclei suggests the effect of the calpain 3 deficiency delays entry into elongation. In addition, in the dKO lens the effect on differentiation and elongation was less pronounced than in the  $\alpha$ 3C $\times$ 46<sup>-/-</sup> mice, suggesting that the loss of the CAPN3 gene can compensate to some extent the lack of  $\alpha$ 3C $\times$ 46. The delayed entry into elongation due to lack of calpain 3 may be responsible for altering the optical properties of the lens that was detected in lenses lacking the calpain 3 gene. A more detailed characterization by electron microscopy may provide further insights into how the differentiation process is affected in the absence of  $\alpha$ 3C $\times$ 46 and/or calpain 3.

The study of a nuclear cataract in mice may be of relevance to human senile cataracts. The senile cataracts in humans also involve proteolysis of crystallins and their aggregation. Cortical cataracts in humans cause light scattering and ionic disturbances including an increase in intracellular Ca<sup>2+</sup> ion.<sup>15</sup> Thus, even though different mechanisms may initiate cataracts, the endpoints may be the same in both transgenic mice and in human senile cataracts. Changes in the ions in the lens are associated with cataractogenesis, and calcium-induced lens opacity is a well characterized model for generation of a cataract.<sup>8,9,15,33-35</sup> Cleavage fragments of  $\gamma$ -crystallin have been detected in human senile cataracts.<sup>11</sup> However, the protease responsible for  $\gamma$ -crystallin cleavage in humans is not known. In both human and mouse models, activation of calpain(s) have been implicated during cataractogenesis.<sup>14,36</sup> Lp82 is the principal protease responsible for cataractogenesis in the  $\alpha$ 3C $\times$ 46<sup>-/-</sup> lens and its activation correlates with the cleavage of  $\gamma$ -crystallin.<sup>8</sup> Our observation of the reduced opacity of the lens and the absence of detectable cleavage of  $\gamma$ -crystallin in the lenses from dKO mice, up to at least 11 weeks is consistent with calpain 3 isoform(s) having a major role in the formation of age-related nuclear cataracts in  $\alpha$ 3C $\times$ 46<sup>-/-</sup> lens. One difference between primates and rodents is that lens preferred Lp82 (major splice variant for calpain 3 in rodents) is believed to be absent in humans,<sup>37</sup> However, it is interesting to note that  $\gamma$ -crystallins, cleaved at sites identical with those

associated with the Lp82-mediated proteolysis of  $\gamma$ -crystallins (between Asp-73 and Ser-74 in rodents<sup>6</sup>), have been identified in human lenses.<sup>38</sup> Furthermore, a novel variant of p94/calpain 3 (hUp84/49) that is expressed ubiquitously has been detected in human lens epithelial cells.<sup>39</sup> P94/calpain 3 has the following unique characteristics, distinct from those of the conventional calpains. Inhibitors of the conventional calpains, including calpastatin and EDTA, have no effect on p94 autolysis.<sup>40</sup> This suggests that either p94/calpain 3 (hUp84/49) or a different calpain 3 isoform may be present in human lenses,<sup>39</sup> and its activation leads to  $\gamma$ -crystallin cleavage as in the mouse models.

As previously reported,  $\alpha$ 3Cx46 is important for calcium homeostasis in the lens. Deletion of  $\alpha$ 3Cx46 gap junctions results in an increase in total calcium in the nuclear region of the lens<sup>8,9</sup> from age 1 week to 4 weeks. In the present study, ion level measurements of the lenses showed a temporal increase in levels of calcium ions in dKO mice similar to that observed in the  $\alpha$ 3Cx46<sup>-/-</sup> mice and reached a plateau at approximately 5 weeks (Fig. 6A). Because a nuclear cataract is readily observable in the  $\alpha$ 3Cx46<sup>-/-</sup> lens at this age, unlike the dKO lens, this result suggests that increased Ca<sup>2+</sup> levels can lead to cataract formation in the lens even in the absence of  $\gamma$ -crystallin cleavage. However, the opacity observed in the lenses of the dKO mice is different in appearance (more diffuse and powdery) from the dense, nuclear cataracts observed in the  $\alpha$ 3Cx46<sup>-/-</sup> mice. The mechanism by which this diffuse cataract is formed is not known. Possibly, it is due to cleavage of other substrates, such as cytoskeletal proteins, rather than crystallins.

Unique to the dKO lens was a two- to threefold increase in Na<sup>+</sup> levels that was observed at 11 weeks (Fig. 6B). Both the wet-dry weight of lenses and water content among WT,  $\alpha$ 3Cx46<sup>-/-</sup>, CAPN3<sup>-/-</sup>, and dKO mice from the age of 4 weeks to 24 weeks were not significantly changed. In addition there was no significant change of water content between the lenses of 8- and 11-week dKO mice (Fig. 1). Furthermore, comparisons of light micrographs of whole lens section did not detect any significant change in gross structure of inner lens fibers between 8- and 11-week-old dKO mice (data not shown). A more detailed characterization by electron microscopy may provide further insights into the structural alterations affected from the lenses of 8- and 11-week-old dKO mice.

The significance, if any, of the increased sodium concentration in dKO mice is not known. Lens sodium concentration increases have been reported previously in hereditary cataract mice<sup>41,42</sup> and in human senile cataract.<sup>43</sup> As the Na<sup>+</sup> moves inward from surface of the lens, it is continuously crossing into fiber cells, driven by its transmembrane electrochemical gradient.<sup>9</sup> Once in the intracellular compartment, it reverses direction and flows from cell-to-cell via gap junctions toward the lens surface. The differentiating fibers have their gap junction coupling conductance concentrated in the equatorial region, so the intracellular current is directed to the equatorial surface epithelial cells. Recent studies<sup>44,45</sup> have shown that Na/K-ATPase activity is highly concentrated at the equatorial surface, where it can transport the intracellular flux of Na<sup>+</sup> out of the lens. Epithelial cells are responsible for essentially all the active transmembrane transport in the lens, including those involving Na/K-ATPase.<sup>46</sup> The activity of Na/K ATPase decreases with increasing age in humans, and this decrease occurs primarily in the inner nuclear region.<sup>47</sup> In experimental and hereditary cataracts in animals, loss in the activity of Na/K-ATPase has been associated with lens opacification.<sup>47</sup> Furthermore, Na/K-ATPase activity decreases in human cataracts. In severe cataractous human lenses, a marked decrease in the Na/K-ATPase activity has been demonstrated in all parts of the lens, in contrast to less severe cataracts, where the decrease in the enzyme activity occurs primarily in the cortical and nuclear regions.<sup>47</sup> Most of the Na/K-ATPase activities occur in epithelial cells of lenses.<sup>46</sup> It is interesting that the opacity of dKO lenses increased between 8 and 11 weeks of age, the same time as the increase in sodium level was observed. It is possible that there is a significant decrease of Na/K-ATPase activity in 11 week dKO mice and that it



leads to more severe cataract compared with the moderate cataract in 8-week-old dKO mice. Duncan et al.<sup>48</sup> have studied the physiological status of human lens membranes of different ages in the population. They found that in human lenses, membrane potentials increased with age. All the older lenses had markedly higher calcium and sodium concentration that increased with age and grade of the cataract. Recently, it has been reported that human lens phospholipid changes with age and cataract.<sup>49</sup> As a result of the elevation of sphingolipid levels with species, age, and cataract, lipid hydrocarbon chain order, or stiffness, increases. Possibly the increased sphingolipid levels reduces calcium pump activity, among its many other effects.

In summary, the present study demonstrates directly that the calpain 3 or its isoforms is necessary for formation of the nuclear cataract that is observed in the  $\alpha 3\text{Cx}46^{-/-}$  lens. In the absence of the CAPN3 gene, the formation of a cataract is delayed, and its appearance is changed to a more diffuse, pulverulent type. The loss of the CAPN3 gene prevents the cleavage of  $\gamma$ -crystallin. The results are consistent with the hypothesis that the loss of  $\alpha 3\text{Cx}46$  leads to increased levels of  $\text{Ca}^{2+}$  ions, and this increase activates the CAPN3 isoform, Lp82/85, which results in the formation of a nuclear cataract. The potential relevance of this mouse model for studying human cataracts is strengthened by the recent report that a human autosomal dominant cataract has been mapped to the same region on human chromosome 13 where the  $\alpha 3\text{Cx}46$  gene is located.<sup>50</sup>

#### Acknowledgements

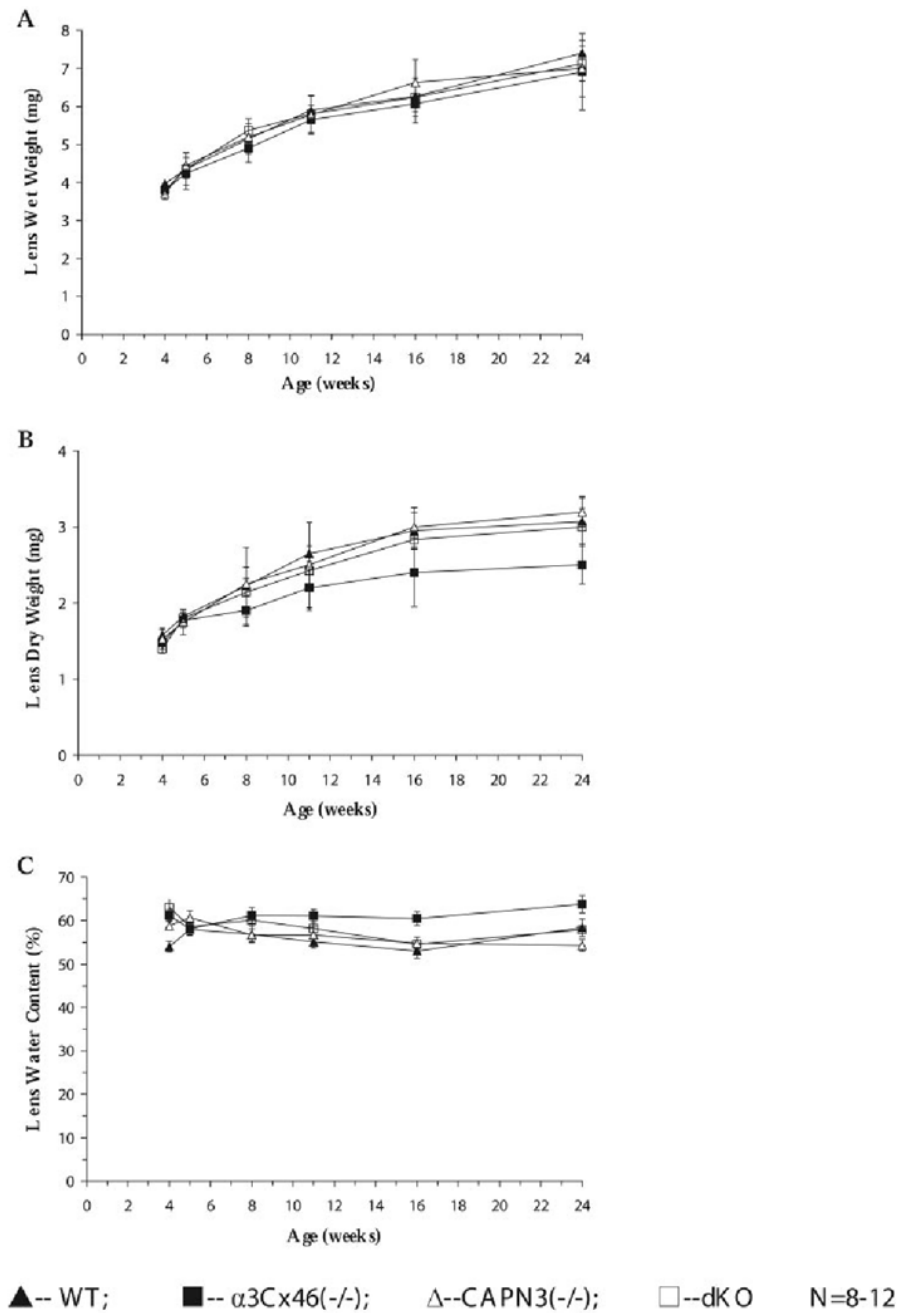
Supported by Grants EY013605 and EY01792 (NMK) and EY06642 to (JRK) from the National Institutes of Health.

#### References

1. Willecke K, Eiberger J, Degen J, et al. Structural and functional diversity of connexin genes in the mouse and human genome. *Biol Chem* 2002;383:725–737. [PubMed: 12108537]
2. Hua VB, Chang AB, Tchieu JH, Kumar NM, Nielsen PA, Saier MH Jr. Sequence and phylogenetic analyses of 4 TMS junctional proteins of animals: connexins, innexins, claudins and occludins. *J Membr Biol* 2003;194:59–76. [PubMed: 14502443]
3. Yancey SB, Biswal S, Revel JP. Spatial and temporal patterns of distribution of the gap junction protein connexin43 during mouse gastrulation and organogenesis. *Development* 1992;114:203–212. [PubMed: 1315676]
4. Paul DL, Ebihara L, Takemoto LJ, Swenson KI, Goodenough DA. Connexin46, a novel lens gap junction protein, induces voltage-gated currents in nonjunctional plasma membrane of *Xenopus* oocytes. *J Cell Biol* 1991;115:1077–1089. [PubMed: 1659572]
5. Church RL, Wang JH, Steele E. The human lens intrinsic membrane protein MP70 (Cx50) gene: clonal analysis and chromosome mapping. *Curr Eye Res* 1995;14:215–221. [PubMed: 7796604]
6. Gong X, Li E, Klier G, et al. Disruption of alpha3 connexin gene leads to proteolysis and cataractogenesis in mice. *Cell* 1997;91:833–843. [PubMed: 9413992]
7. Gong X, Agopian K, Kumar NM, Gilula NB. Genetic factors influence cataract formation in alpha 3 connexin knockout mice. *Dev Genet* 1999;24:27–32. [PubMed: 10079508]
8. Baruch A, Greenbaum D, Levy ET, et al. Defining a link between gap junction communication, proteolysis, and cataract formation. *J Biol Chem* 2001;276:28999–29006. [PubMed: 11395508]
9. Gao J, Sun X, Martinez-Wittinghan FJ, Gong X, White TW, Mathias RT. Connections between connexins, calcium, and cataracts in the lens. *J Gen Physiol* 2004;124:289–300. [PubMed: 15452195]
10. Duncan G, Jacob TJ. Calcium and the physiology of cataract. *Ciba Found Symp* 1984;106:132–152. [PubMed: 6096095]
11. Sandberg HO, Closs O. The alpha and gamma crystallin content in aqueous humor of eyes with clear lenses and with cataracts. *Exp Eye Res* 1979;28:601–610. [PubMed: 446578]
12. Pal JD, Liu X, Mackay D, et al. Connexin46 mutations linked to congenital cataract show loss of gap junction channel function. *Am J Physiol* 2000;279:C596–C602.

13. Minogue PJ, Liu X, Ebihara L, Beyer EC, Berthoud VM. An aberrant sequence in a connexin46 mutant underlies congenital cataracts. *J Biol Chem* 2005;280:40788–40795. [PubMed: 16204255]
14. Biswas S, Harris F, Dennison S, Singh J, Phoenix DA. Calpains: targets of cataract prevention? *Trends Mol Med* 2004;10:78–84. [PubMed: 15102361]
15. Tang D, Borchman D, Yappert MC, Vrensen GG, Rasi V. Influence of age, diabetes, and cataract on calcium, lipid-calcium, and protein-calcium relationships in human lenses. *Invest Ophthalmol Vis Sci* 2003;44:2059–2066. [PubMed: 12714644]
16. Ma H, Fukiage C, Azuma M, Shearer TR. Cloning and expression of mRNA for calpain Lp82 from rat lens: splice variant of p94. *Invest Ophthalmol Vis Sci* 1998;39:454–461. [PubMed: 9478008]
17. Ma H, Hata I, Shih M, et al. Lp82 is the dominant form of calpain in young mouse lens. *Exp Eye Res* 1999;68:447–456. [PubMed: 10192802]
18. Ma H, Shih M, Fukiage C, et al. Influence of specific regions in Lp82 calpain on protein stability, activity, and localization within lens. *Invest Ophthalmol Vis Sci* 2000;41:4232–4239. [PubMed: 11095620]
19. Nakamura Y, Fukiage C, Shih M, et al. Contribution of calpain Lp82-induced proteolysis to experimental cataractogenesis in mice. *Invest Ophthalmol Vis Sci* 2000;41:1460–1466. [PubMed: 10798663]
20. Tamada Y, Fukiage C, Mizutani K, et al. Calpain inhibitor, SJA6017, reduces the rate of formation of selenite cataract in rats. *Curr Eye Res* 2001;22:280–285. [PubMed: 11462167]
21. Richard I, Roudaut C, Marchand S, et al. Loss of calpain 3 proteolytic activity leads to muscular dystrophy and to apoptosis-associated IkappaBalpha/nuclear factor kappaB pathway perturbation in mice. *J Cell Biol* 2000;151:1583–1590. [PubMed: 11134085]
22. Kuszak JR, Sivak JG, Weerheim JA. Lens optical quality is a direct function of lens sutural architecture. *Invest Ophthalmol Vis Sci* 1991;32:2119–2129. [PubMed: 2055702]
23. Sivak JG, Herbert KL, Peterson KL, Kuszak JR. The interrelationship of lens anatomy and optical quality. I. Non-primate lenses. *Exp Eye Res* 1994;59:505–520. [PubMed: 9492753]
24. Shiels A, Bassnett S, Varadaraj K, et al. Optical dysfunction of the crystalline lens in aquaporin-0-deficient mice. *Physiol Genomics* 2001;7:179–186. [PubMed: 11773604]
25. Al-Ghoul KJ, Kirk T, Kuszak AJ, Zoltoski RK, Shiels A, Kuszak JR. Lens structure in MIP-deficient mice. *Anat Rec* 2003;273A:714–730.
26. Nielsen PA, Baruch A, Shestopalov VI, et al. Lens connexins alpha3Cx46 and alpha8Cx50 interact with zonula occludens protein-1 (ZO-1). *Mol Biol Cell* 2003;14:2470–2481. [PubMed: 12808044]
27. Xi J, Farjo R, Yoshida S, et al. A comprehensive analysis of the expression of crystallins in mouse retina. *Mol Vis* 2003;9:410–419. [PubMed: 12949468]
28. Rao PV, Huang QL, Horwitz J, et al. Evidence that  $\alpha$ -crystallin prevents non-specific protein aggregation in the intact eye lens. *Biochim Biophys Acta* 1995;1245:439–447. [PubMed: 8541324]
29. Brady JP, Garland D, Douglas-Tabor Y, et al. Targeted disruption of the mouse  $\alpha$ A-crystallin gene induces cataract and cytoplasmic inclusion bodies containing the small heat shock protein  $\alpha$ B-crystallin. *Proc Natl Acad Sci USA* 1997;94:884–889. [PubMed: 9023351]
30. Takemoto L. Release of  $\alpha$ A sequence 158–173 correlates with a decrease in the molecular chaperone properties of native  $\alpha$ -crystallin. *Exp Eye Res* 1994;59:239–242. [PubMed: 7835414]
31. Ueda Y, Fukiage C, Shih M, et al. Mass measurements of C-terminally truncated alpha-crystallins from two-dimensional gels identify Lp82 as a major endopeptidase in rat lens. *Mol Cell Proteomics* 2002;1:357–365. [PubMed: 12118077]
32. Harrington V, McCall S, Huynh S, et al. Crystallins in water soluble high molecular weight protein fractions and water insoluble protein fractions in aging and cataractous human lenses. *Mol Vis* 2004;10:476–489. [PubMed: 15303090]
33. Duncan G, van Heyningen R. Distribution of non-diffusible calcium and sodium in normal and cataractous human lenses. *Exp Eye Res* 1977;25:183–193. [PubMed: 913509]
34. Hightower KR. Cytotoxic effects of internal calcium on lens physiology: a review. *Curr Eye Res* 1985;4:453–459. [PubMed: 2990821]

35. Sanderson J, Marcantonio JM, Duncan G. A human lens model of cortical cataract: Ca<sup>2+</sup>-induced protein loss, vimentin cleavage and opacification. *Invest Ophthalmol Vis Sci* 2000;41:2255–2261. [PubMed: 10892870]
36. Sanderson J, Marcantonio JM, Duncan G. Calcium ionophore induced proteolysis and cataract: inhibition by cell permeable calpain antagonists. *Biochem Biophys Res Commun* 1996;218:893–901. [PubMed: 8579611]
37. Fougerousse F, Bullen P, Herasse M, et al. Human-mouse differences in the embryonic expression patterns of developmental control genes and disease genes. *Hum Mol Genet* 2000;9:165–173. [PubMed: 10607827]
38. Srivastava OP, Srivastava K. Degradation of gamma D- and gamma s-crystallins in human lenses. *Biochem Biophys Res Commun* 1998;253:288–294. [PubMed: 9878530]
39. Kawabata Y, Hata S, Ono Y, et al. Newly identified exons encoding novel variants of p94/calpain 3 are expressed ubiquitously and overlap the alpha-glucosidase C gene. *FEBS Lett* 2003;555:623–630. [PubMed: 14675785]
40. Sorimachi H, Toyama-Sorimachi N, Saido TC, et al. Muscle-specific calpain, p94, is degraded by autolysis immediately after translation, resulting in disappearance from muscle. *J Biol Chem* 1993;268:10593–10605. [PubMed: 8486713]
41. Kuck JF, Kuck KD. The Emory mouse cataract: loss of soluble protein, glutathione, protein sulfhydryl and other changes. *Exp Eye Res* 1983;36:351–362. [PubMed: 6832231]
42. Kador PF, Fukui HN, Fukuishi S, et al. Philly mouse: a new model of hereditary cataract. *Exp Eye Res* 1980;30:59–68. [PubMed: 7363969]
43. Dilsiz N, Olcucu A, Atas M. Determination of calcium, sodium, potassium and magnesium concentrations in human senile cataractous lenses. *Cell Biochem Funct* 2000;18:259–262. [PubMed: 11180288]
44. Gao J, Sun X, Yatsula V, et al. Isoform-specific function and distribution of Na/K pumps in the frog lens epithelium. *J Membr Biol* 2000;178:89–101. [PubMed: 11083898]
45. Tamiya S, Dean WL, Paterson CA, et al. Regional distribution of Na,K-ATPase activity in porcine lens epithelium. *Invest Ophthalmol Vis Sci* 2003;44:4395–4399. [PubMed: 14507885]
46. Paterson CA, Delamere NA. ATPases and lens ion balance. *Exp Eye Res* 2004;78:699–703. [PubMed: 15106949]
47. Kobatashi S, Roy D, Spector A. Sodium/potassium ATPase in normal and cataractous human lenses. *Curr Eye Res* 1983;2:327–334. [PubMed: 6299650]
48. Duncan, G.; Marcantonio, JM.; Tomlinson, J. Lens Calcium and cataract. In: Obrecht, G.; Lawrence, WS., editors. *Molecular Biology of the Lens*. New York: Plenum Press; 1991. p. 33-40.
49. Huang L, Grami V, Marrero Y, et al. Human lens phospholipid changes with age and cataract. *Invest Ophthalmol Vis Sci* 2005;46:1682–1689. [PubMed: 15851569]
50. Mackay D, Ionides A, Berry V, et al. A new locus for dominant “zonular pulverulent” cataract, on chromosome 13. *Am J Hum Genet* 1997;60:1474–1478. [PubMed: 9199569]

**FIGURE 1.**

Comparisons of the total wet, dry weight, and water content of lenses of WT,  $\alpha3Crx46^{-/-}$ , CAPN3 $^{-/-}$ , and dKO mice as a function of age. Lenses were weighed immediately after dissection from the eye. The lens weight and water content in the figure represents an average of lens from 8 to 12 mice. Data represent the total lens weight of ( $\blacktriangle$ ) WT, ( $\blacksquare$ )  $\alpha3Crx46^{-/-}$ , ( $\triangle$ ) CAPN3 $^{-/-}$ , and ( $\square$ ) dKO lenses, respectively. (A) Comparisons of the total wet lens weight. (B) Comparisons of the total dry lens weight. (C) Comparisons of the water content.

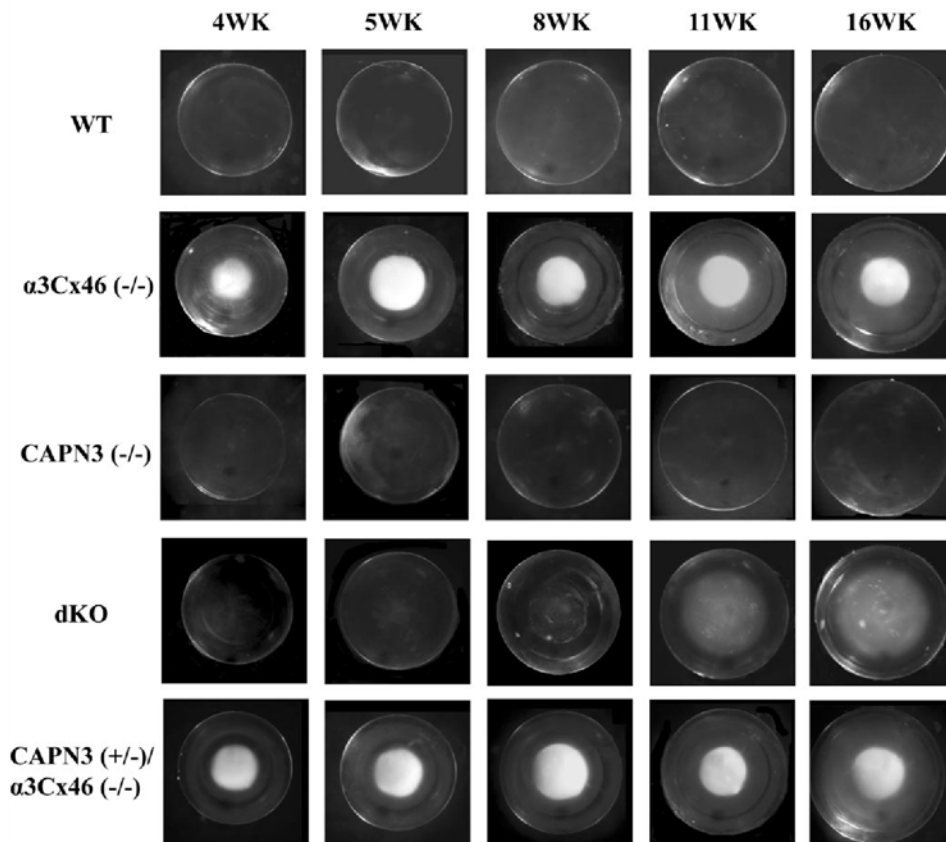


**FIGURE 2.**

Visual examination of lenses from the different KO mice. Shown are lenses dissected from fresh eyes of WT,  $\alpha 3\text{Cx46}^{-/-}$ , CAPN3<sup>-/-</sup>, dKO, and CAPN3<sup>+/-</sup>/ $\alpha 3\text{Cx46}^{-/-}$  mice at the age of 4, 5, 8, 11, and 16 weeks and photographed with a dissection microscope. Note that cataract formation in the dKO mouse lens is delayed and its appearance is changed compared to the  $\alpha 3\text{Cx46}^{-/-}$  mice.

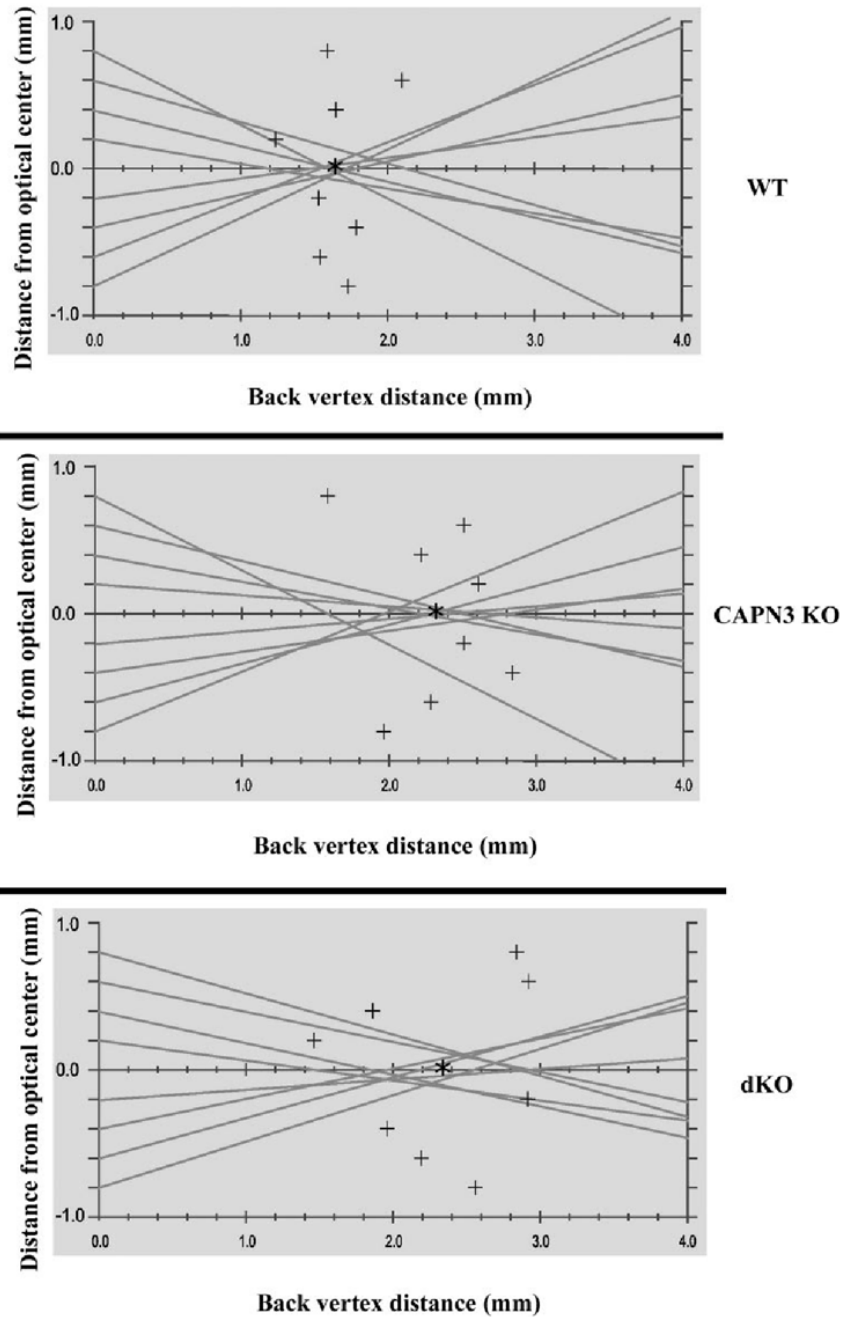


**FIGURE 3.**

Representative laser scan profiles from the different KO mouse lenses. Shown are a typical profile of lenses from 7.5-week-old wild-type, CAPN3<sup>-/-</sup>, and dKO mice. *Lines*: the pathway of the laser beam and the data points (+) represent the focal point of each beam. The average BVD (*asterisk*) is calculated from averaging the value of each of these data points, whereas the variability in the BVD is the SEM. Both CAPN3<sup>-/-</sup> and dKO lenses showed an increase in the average BVD, as well as an increase in the scatter of the data points around each of the means.

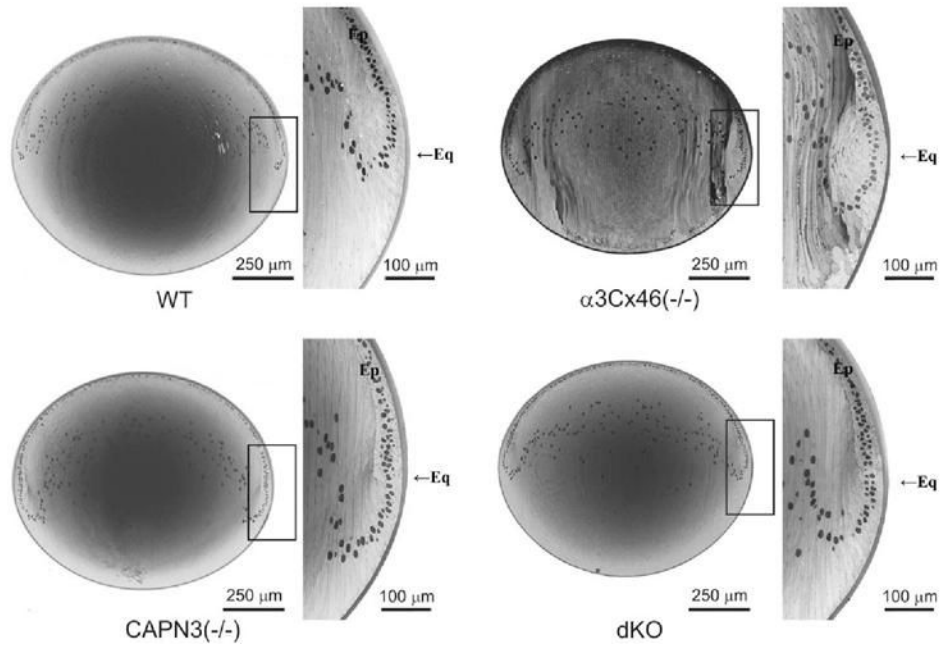


**FIGURE 4.**

Light micrographs of the whole lens section and magnified equatorial region from 8-week-old wild-type,  $\alpha 3\text{Crx}46^{-/-}$ , CAPN3 $^{-/-}$ , and dKO lenses. The epithelial (Ep) differentiation zone was profoundly altered in the  $\alpha 3\text{Crx}46^{-/-}$  lenses such that the cells had a delayed and abnormal entry into the elongation process in the immature cortex. In the CAPN3 $^{-/-}$  lens, the epithelial differentiation zone was slightly altered, but the elongation process appeared to be normal. Last, the effects of the original deficiency were partially reversed in the dKO lens. Eq, equator.

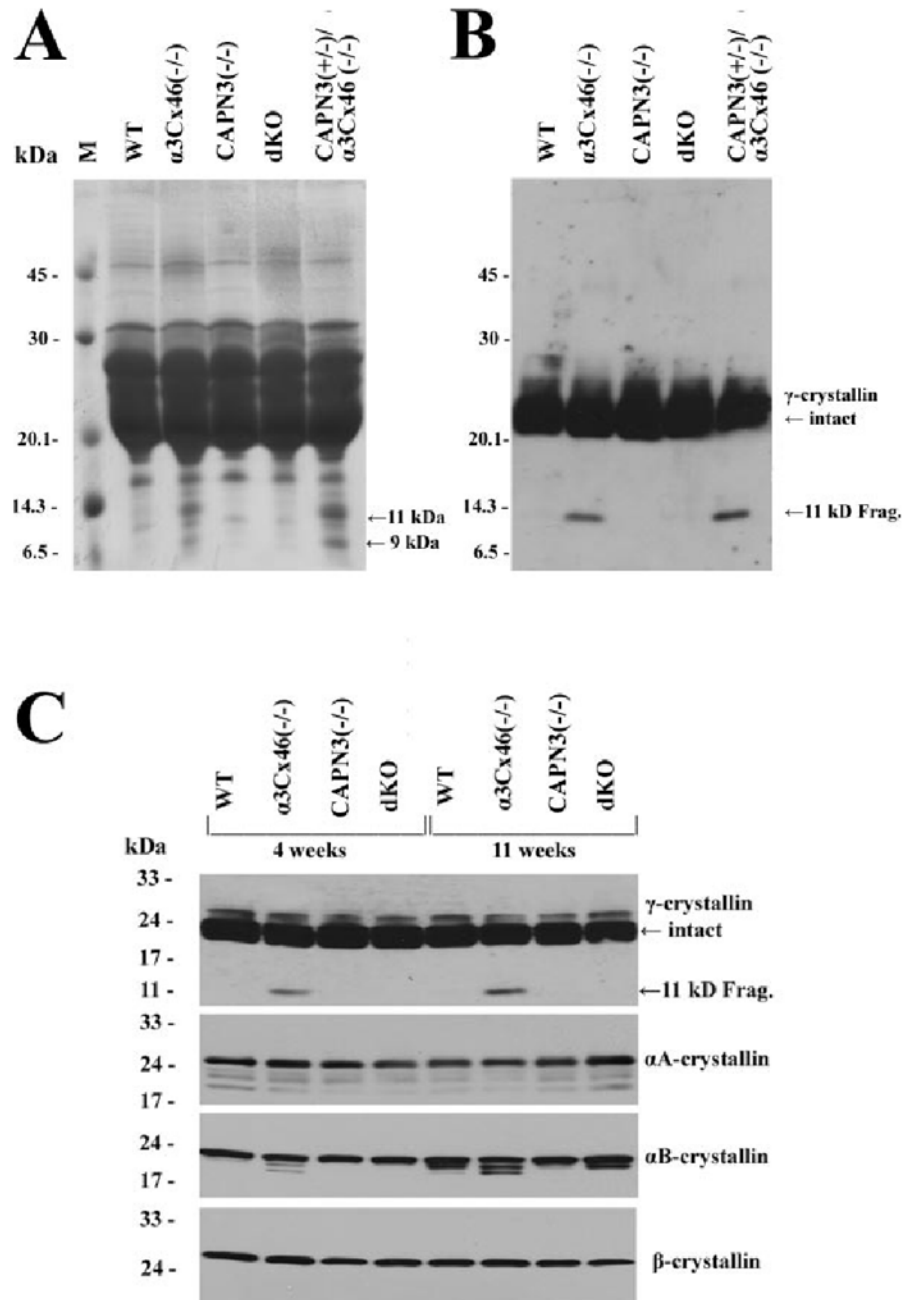


**FIGURE 5.**

Analysis of crystallins in the lenses from the different mice. **(A)** A Coomassie blue–stained gel of the total lens homogenate from 11-week-old lenses of WT,  $\alpha3Crx46^{-/-}$ ,  $CAPN3^{-/-}$ , dKO, and  $CAPN3^{+/-}/\alpha3Crx46^{-/-}$  mice. Equal amounts of the samples (200  $\mu$ g) were separated on a 15% SDS-polyacrylamide gel and stained with Coomassie blue. *Arrows*: the bands (in lanes of  $\alpha3Crx46^{-/-}$  or  $CAPN3^{+/-}/\alpha3Crx46^{-/-}$  samples) corresponding to the 9- and 11-kDa cleaved forms of  $\gamma$ -crystallins. **(B)** Western blot analysis of samples used for **(A)**. Equal amounts of the total homogenate samples (5  $\mu$ g) were subjected to 15% SDS-PAGE and Western blot analysis. An anti- $\gamma$ -crystallin polyclonal antibody was used. *Arrows*: position of the intact and cleaved form of  $\gamma$ -crystallin protein. **(C)** Crystallin profiles in the lenses of the different KO mice.



Homogenates from WT,  $\alpha 3\text{Cx}46^{-/-}$ ,  $\text{CAPN}3^{-/-}$ , and dKO lenses were prepared from mice of 4 or 11 weeks of age. Equal amounts of the total homogenate samples ( $5\ \mu\text{g}$  for  $\gamma$ -crystallins and  $10\ \mu\text{g}$  for other crystallins) were subjected to 10% to 20% gradient SDS-PAGE and Western blot analysis. Four different antibodies—anti- $\gamma$ -, anti- $\alpha\text{A}$ -, anti- $\alpha\text{B}$ -, and anti- $\beta$ -crystallins—were used to analyze the samples by Western blot analysis. *Arrows*: position of the intact and cleaved form of  $\gamma$ -crystallin protein.

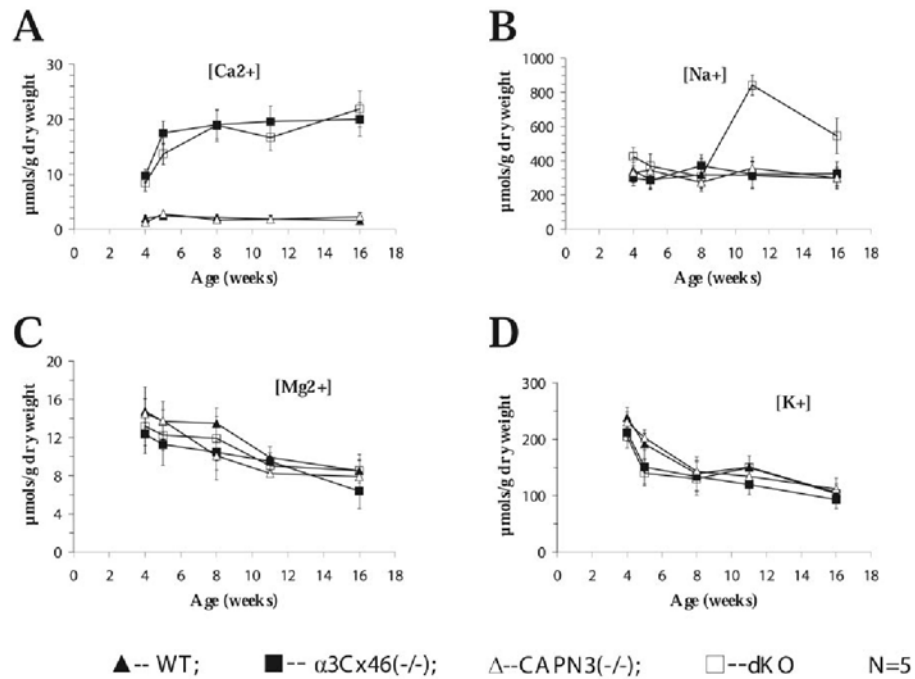


**FIGURE 6.** Calcium accumulates in the lenses of both  $\alpha$ 3C<sub>x</sub>46 and dKO mice. Lenses from WT,  $\alpha$ 3C<sub>x</sub>46<sup>-/-</sup>, CAPN3<sup>-/-</sup>, and dKO at the indicated ages were vacuum-dried, weighed, and solubilized in 2% nitric acid for 12 hours. The content of (A) calcium, (B) sodium, (C) magnesium, and (D) potassium was determined by atomic emission spectroscopy. All measurements were normalized to lens dry weight. N, number of mice analyzed in each experiment.

**TABLE 1**  
Optical Properties of Lenses of Knockout Mice Compared with Those of Wild-Type Mice

	Wild- Type	CAPN3 KO	dKO
<i>n</i>	8	6	6
Average BVD (mm)	1.50 ± 0.12	2.69 ± 0.10 <sup>*</sup>	2.27 ± 0.15 <sup>*†</sup>
BVD variability	0.170 ± 0.005	0.365 ± 0.036 <sup>*</sup>	0.397 ± 0.097 <sup>*</sup>

<sup>\*</sup> *P* < 0.05 as compared to wild-type mice.

<sup>†</sup> *P* < 0.05 as compared to calpain 3 KO mice.